Title

Transport matrix for particles and momentum in collisional drift waves turbulence in linear plasma devices

Journal

Physics of Plasmas, 23(2)

ISSN

1070-664X

Authors

Ashourvan, Arash
Diamond, PH
Gürcan, ÖD

Publication Date

2016-02-01

DOI

10.1063/1.4942420

Transport matrix for particles and momentum in collisional drift waves turbulence in linear plasma devices

Arash Ashourvan, P. H. Diamond, and Ö. D. Gürcan

Citation: Physics of Plasmas **23**, 022309 (2016); doi: 10.1063/1.4942420
View online: http://dx.doi.org/10.1063/1.4942420
View Table of Contents: http://scitation.aip.org/content/aip/journal/pop/23/2?ver=pdfcov
Published by the AIP Publishing

Transport matrix for particles and momentum in collisional drift waves turbulence in linear plasma devices

Arash Ashourvan,[1,2] P. H. Diamond,[1,2,3] and Ö. D. Gürcan[4]
[1]Center for Momentum Transport and Flow Organization, University of California San Diego, La Jolla, California 92093, USA
[2]Center for Energy Research, University of California San Diego, La Jolla, California 92093, USA
[3]Center for Astrophysics and Space Sciences (CASS) and Department of Physics, University of California San Diego, La Jolla, California 92093, USA
[4]Laboratoire de Physique des Plasmas, Ecole Polytechnique, Palaiseau, France

(Received 23 September 2015; accepted 8 February 2016; published online 29 February 2016)

The relationship between the physics of turbulent transport of particles and azimuthal momentum in a linear plasma device is investigated using a simple model with a background density gradient and zonal flows driven by turbulent stresses. Pure shear flow driven Kelvin-Helmholtz instabilities ($k_{\|} = 0$) relax the flow and drive an outward (down gradient) flux of particles. However, instabilities at finite $k_{\|}$ with flow enhanced pumping can locally drive an inward particle pinch. The turbulent vorticity flux consists of a turbulent viscosity term, which acts to reduce the global vorticity gradient and the residual vorticity flux term, accelerating the zonal flows from rest. Moreover, we use the positivity of the production of fluctuation potential enstrophy to obtain a constraint relation, which tightly links the vorticity transport to the particle transport. This relation can be useful in explaining the experimentally observed correlation between the presence of $E \times B$ flow shear and the measured inward particle flux in various magnetically confined plasma devices. © *2016 AIP Publishing LLC*. [http://dx.doi.org/10.1063/1.4942420]

I. INTRODUCTION

The self regulating, self-consistent "predator-pray" feedback loop character of the zonal flow-turbulence system has been well established in various experiments[1,2] and numerical simulations.[3] In its most basic form, the parameters controlling this system are the sources and zonal flow (ZF) damping. In the presence of flow, the turbulence level, which determines the transport, is directly set by the flow damping.[4] In the low collisionality limit, there have been some efforts towards the understanding of the zonal flow saturation mechanisms.[5,6] However, collisionless damping and saturation of ZF are still not well understood and saturated ZF profiles cannot be accurately predicted. In linear cylindrical plasma devices, due to their relatively smaller size and simpler geometry, controlling the equilibrium parameters of the plasma is convenient. This facilitates a close examination of the turbulence-ZF system, identification of collisionless saturation mechanisms and investigation of the impact of such mechanisms on transport, in the absence of toroidal effects.

In the fusion community, what mainly drives the interest in ZFs is that such flows, as well as externally driven, mean $E \times B$ flows, have been linked to triggering the formation of transport barriers by reducing the turbulence and transport. During or shortly after the formation of transport barriers, net inward turbulent particle fluxes have been observed.[7–10] This inward turbulent particle flux has also been observed in the Large Plasma Device (LAPD)[11,12] when a strong externally applied $E \times B$ flow shear was induced, and in the CSDX[13] linear machine with the spontaneous formation of shear (zonal) flows. Hence, these observations motivate an interest in the connection between $E \times B$ flow shear and the physics of the inward particle pinch.

In a wide range of turbulent systems (e.g., biochemical systems,[14] atmospheric systems,[15] magnetically confined space plasmas,[16–21] and controlled fusion systems[22–26]), the down-gradient diffusive transport fluxes act to relax the system towards an equilibrium state. Non-diffusive transport fluxes, such as the turbulent particle pinch, the momentum pinch, and the residual stress, can play a role in maintaining non-equilibrium profile conditions.[27,28] For some cases, the turbulent particle pinch may be large enough such that it can overcome outward diffusive transport and result in a net up-gradient, inward turbulent particle flux.

This paper has three principal foci: inward particle flux, shear flow generation, and their relation. Regarding inward fluxes, for magnetic fusion confinement devices, there has been an interest in the inward particle flux as a means for possibly controlling the plasma density and thus controlling the transport properties. Peaking of the density can result in a significant enhancement of confinement quality and a significant improvement of the fusion power (higher pedestal pressure in H-mode). Coppi and Spight in Ref. 29 proposed a theoretical model for driving an inward pinch generated by ion mixing mode turbulence, resulting from neutral gas injection. More recently, another mechanism was proposed in Ref. 30, in which the instabilities driven by the parallel shear flows along the magnetic field lines can drive and inward pinch of particles. These parallel flow shears can be driven by drift wave turbulence through the residual stress resulting from broken parallel symmetry.[27,31,32] However, despite these analyses, comparisons of the CSDX data[33,34] with models indicate the need for further studies.

Regarding the ZF formation, Hasegawa and Wakatani pointed out that this particularly simple system conserves energy and potential vorticity, the latter which leads to the spontaneous generation of ZF by turbulence (Reynolds stress). The model that Hasegawa and Wakatani[35,36](HW model) presented is a simple 2D system describing the collisional drift wave instability driven turbulence. This work was an extension on the previous model of nonlinear electrostatic turbulence by Hasegawa and Mima,[37] which is isomorphic to the quasi-geostrophic or Rossby wave equation first derived by Charney.[38,39] The pioneering work on ZF self-generation in the HW system[35,36] was followed by the observation of turbulence-driven ZF in the nonlinear simulations of various fluid turbulence models.[40–44]

Residual stresses can also drive a flow by tapping into the free energy sources of pressure or density gradient.[27] Following the presentation of the theoretical model on residual stress driven flow in Ref. 27, this work was successfully compared to the experiments performed on the CSDX linear plasma device in Ref. 28, demonstrating that the residual stress at the plasma-wall boundary drives a shear azimuthal flow at the plasma edge. Furthermore, the flow shear is spread to the core region via the turbulent diffusion, resulting in a net motion of plasma without an outside torque source. In this paper, we develop the analytical theory of residual stress and also discuss the relation of shear flow to the inward flux.

In this paper, we investigate the competition between down and up gradient particle transport and its relation to anomalous momentum transport in a linear plasma device with a straight, uniform magnetic field. Moreover, we discuss the dependence of the particle and vorticity fluxes on the background flow and density profiles. Naturally, in this work, the complexities arising from the toroidal geometry, i.e., magnetic curvature and magnetic shear have been neglected. We present a mechanism for driving a local net inward particle flux, based on a simple Modified Hasegawa-Wakatani[45] model with both the turbulent stress driven, quasi-equilibrium background flow shear and a background density gradient. Moreover, we derive quasilinear expressions for the local particle flux and vorticity flux. The Taylor identity relates the vorticity flux to the turbulent Reynolds stress (see Eq. (46)). In fact, the negative of the vorticity flux is simply the turbulent force exerted on the flow. The expressions we obtain for both particle and vorticity flux are in general complicated functions of the flow profile and contain diffusive and non-diffusive flux terms, like convective particle pinch (in particle flux) and residual stress (in vorticity flux). The pinch component of the particle flux is extremely sensitive to local flow velocity, which significantly changes with radius. This change in the flow velocity explains why the particle flux is outward in some regions and inward in other regions. More generally, the structure of the particle and momentum fluxes highlights the strong and non-trivial coupling between these two.

Here, we must mention that the traditional quasilinear approach, although a very useful tool in the weak turbulence regimes, has limitations and shortcomings. For example, such phenomena as intermittency and coherent structures, which result from spatial and temporal correlations in the turbulence, cannot be recovered by the quasilinear method. Moreover, nonlinear instabilities[46,47] and the advection of turbulence from unstable into linearly stable regions[48,49] are excluded from the traditional quasilinear approach.

In this minimal model, both axially symmetric ($k_\| = 0$) and non-axially symmetric ($k_\| \neq 0$) instabilities can be driven ($k_\|$ is the axial mode number). Axially symmetric ($k_\| = 0$) modes of this system are Kelvin-Helmholtz (KH) instabilities which do not tap into the free energy in the density gradient and are only driven by the flow shear. The electrostatic potential of the KH modes ($k_\| = 0$) satisfies the well known Rayleigh's eigenvalue equation, which has been extensively discussed in the fluid mechanics literature. The non-axially symmetric ($k_\| \neq 0$) modes can be driven by both the flow shear and the density gradient. Thus, we call these ($k_\| \neq 0$) modes drift-KH instabilities.

We find that the particle flux related to KH modes ($k_\| = 0$) is always in the outward direction, and an inward particle pinch can be carried by the drift-KH ($k_\| \neq 0$) modes. The physical mechanism which can drive this inward pinch is the flow enhanced pumping due to the Doppler effect, which can locally overcome the relaxation-driven diffusive outward flux for some conditions, which we will discuss in this paper.

Moreover, we discuss the energetics of this model, and specifically, we study the transfer of energy between turbulence and flow shear, as a function of the parameters in the system. Here, the energy transfer is quasilinear and does not include higher order (three-wave) interactions. We observe that the energy transfer is from the flow to the turbulence for modes with long wave-lengths compared to the length scale of the flow shear ($k_m^{-1} < q_x^{-1}$, where k_m is the azimuthal wave number and $q_x = 1/L_{ZF}$ is the characteristic ZF wave number). For $k_m^{-1} \approx q_x^{-1}$, direction of energy transfer is from the flow to the turbulence for small amplitude flows, and changes sign as the flow amplitude passes a threshold. For small wave-length modes, the direction of energy transfer is from the turbulence to the flow ($k_m^{-1} > q_x^{-1}$).

Figure 1(a) is a schematic diagram of the energy transfer between ∇n_0, ZF, KH modes ($k_\| = 0$) and drift-KH modes ($k_\| \neq 0$). The arrows in the diagram show the direction of transfer of energy. Zonal flows (produced by ∇n_0 driven by drift waves) provide the free energy to drive linear, pure KH modes. The direction of energy transfer is always from ZFs to pure KH. Figure 1(b) is a schematic diagram showing the growth rate (γ_{growth}) versus the inverse length-scale (wave-number). Typically, growth rates of $k_\| = 0$ modes are larger than the growth rates of the drift-KH modes, since $k_\| = 0$ modes are not screened by Boltzmann electrons and have lower effective inertia than the drift-KH modes do. However, the pure KH modes are not unstable for all flow structures. For $k_\| = 0$ modes, the direction of the turbulent particle flux is always down the density gradient (outward). Zonal flows can also drive linear drift-KH modes ($k_\| \neq 0$) with smaller mode numbers ($k_\perp < q_x$). The direction of the particle flux for these modes can be locally inward ($\Gamma < 0$) or outward ($\Gamma > 0$), depending on the mode frequency and the radial structure of the flow (see Eq. (25)). The drift-KH modes at larger mode numbers ($k_\perp > q_x$) can accelerate the

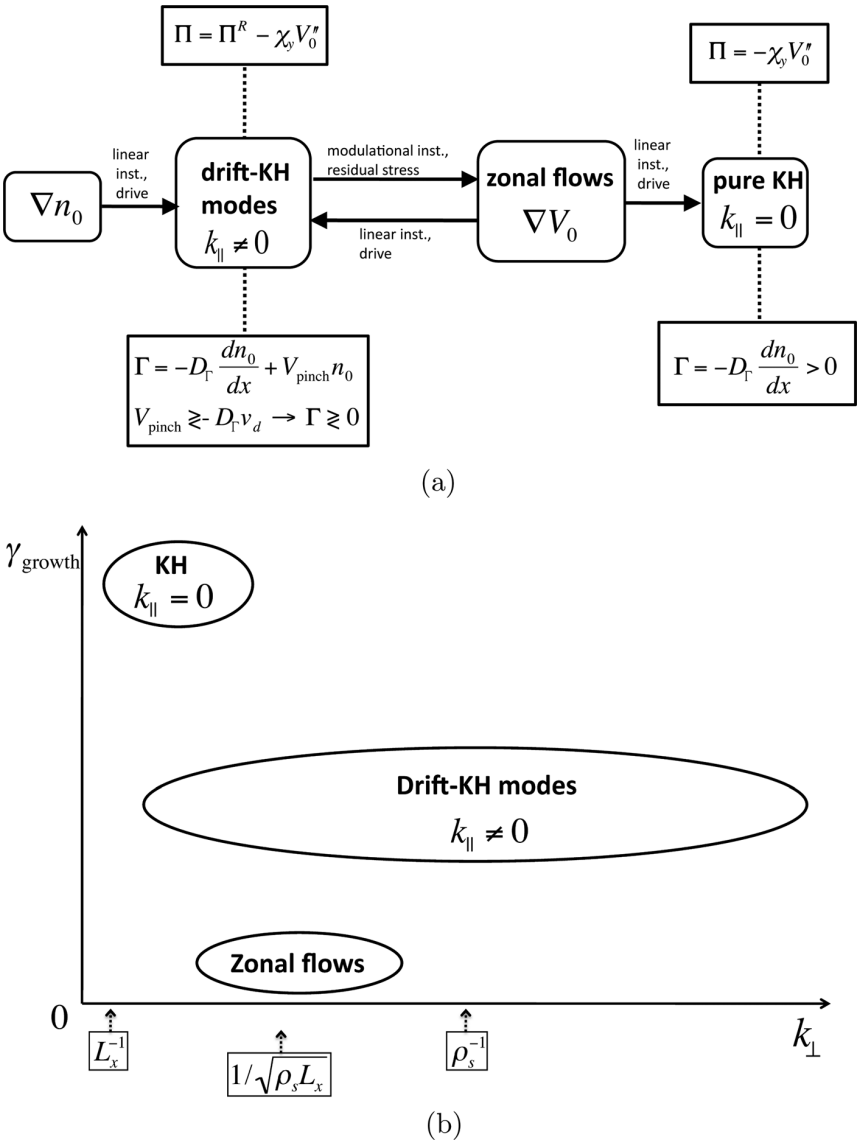

FIG. 1. (a) Diagram of energy transfer between ∇n_0, zonal flow, KH modes ($k_\| = 0$), and drift-KH modes ($k_\| \neq 0$). (b) Schematic distribution of the growth rate (γ_{growth}) versus inverse length-scale (wave number) for zonal flows, drift-KH modes, and pure KH modes.

ZF to larger flow amplitudes via modulational instability (nonlinear) and residual stress (quasilinear). We must note that extensive literature on the theory-numerical[50,51] studies, as well as experimental studies of ZF generation exists for cylindrical, straight field plasmas devices. The direction of the particle flux for these modes is in the outward direction. We must also mention that the drift-KH modes can also drive the generalized KH modes (not depicted in the diagram). These are axially symmetric ($k_\| = 0$) modes which are generated via modulation instability and have growth rates similar to or smaller than those of ZF.[52]

The remainder of this paper is organized as follows: in Section II, we describe the modified Hasegawa-Wakatani model in a slab geometry with a magnetic field in the z direction. In Section III, we obtain relations for quasilinear fluxes of particle and vorticity and the condition for net inward flux. In Section IV, using the fact that the potential enstrophy of the fluctuations is positive definite, we obtain a constraint relation, which tightly links the fluxes of vorticity and particle. In Section V, we obtain the linear eigenvalue equation for the modified Hasegawa-Wakatani system and study the stability of the eigenmodes, using a given ZF profile, constant in time. We calculate the quasilinear flux of particles for the obtained eigenmode solutions and study their functional dependence on flow amplitude and azimuthal mode number. Moreover, we obtain the turbulence energy evolution equation and study the energy transfer between the turbulence and the sources of free energy (i.e., the density and the flow shear), using the linear solutions obtained.

II. MODIFIED HASEGAWA-WAKATANI MODEL

Here, we study a cold ion, quasi-neutral Hasegawa-Wakatani model with temporally and spatially varying density n and electric potential ϕ in the presence of an azimuthal (i.e., along $\hat{y}$) flow velocity profile V_0. Both the flow and the density profile n_0 vary only in the radial ($\hat{x}$) direction. The geometry of the system is taken to be slab of cubic dimensions $0 \leq x \leq L_x$, $0 \leq y \leq L_y$, $0 \leq z \leq L_z$, with the magnetic field pointing in the axial ($\hat{z}$) direction. In the

perpendicular plane, $\hat{y}$ is the direction of symmetry. The electric potential consists of a time dependent fluctuating part $\delta\phi(x,y,z;t)$, plus the quasi-equilibrium flow potential $\phi_0(x)$

$$\hat{\phi} = \delta\hat{\phi}(x,y,z;t) + \hat{\phi}_0(x), \tag{1}$$

where $\hat{\phi} = e\phi/T_e$ is the non-dimensional electric potential. The flow velocity is given by

$$V_0(x) = \partial_x\hat{\phi}_0(x). \tag{2}$$

We scale the spatial dimensions to ρ_s and time to ω_{ci}^{-1}

$$\tilde{x} = x/\rho_s, \quad \tilde{y} = y/\rho_s, \quad \tilde{z} = z/\rho_s, \quad \tilde{t} = \omega_{ci}t. \tag{3}$$

From here forward, we drop the tilde symbol from space and time variables for notational convenience. The linearized form of the evolution equations for the electric potential and the density, in terms of fluctuations $\delta\hat{n}$ and $\delta\hat{\phi}$, is given by Eqs. (A8) and (A9) in the Appendix. Furthermore, we make the assumption that V_0 is a *zonal* flow. Turbulence-driven ZF have a broad range of radial scales, spanning the micro-scale (coherence length of turbulence $\sim$several ρ_s) through the meso-scales (i.e., a fraction of L_x)[53]

$$\rho_s^2 < L_{ZF}^2 \leq L_x\rho_s. \tag{4}$$

As a result, neglecting the terms in Eqs. (A8) and (A9), which vary over the macro-scale $|\partial_x n_0/n_0| = L_n \sim L_x$ in comparison to the flow scaling, these equations are given by

$$(\partial_t + V_0\partial_y)\nabla^2\delta\hat{\phi} + \delta\hat{v}_x\partial_x^2 V_0 = D_\parallel\nabla_\parallel^2(\delta\hat{n} - \delta\hat{\phi}) - \mu\nabla^2\nabla^2\delta\hat{\phi}, \tag{5}$$

$$(\partial_t + V_0\partial_y)\delta\hat{n} - \delta\hat{v}_x v_d = D_\parallel\nabla_\parallel^2(\delta\hat{n} - \delta\hat{\phi}) - D_n\nabla^2\delta\hat{n}, \tag{6}$$

where we defined $\delta\hat{n} = \delta n/n_0$ and the non-dimensional electron drift velocity is defined as

$$v_d(x) = -d\ln n_0/dx, \tag{7}$$

μ and D_n are viscosity related diffusion coefficients for vorticity and density. From here forward, we neglect the viscous diffusion terms and we will explore the effects of viscosity on stability in a future paper. We assume unstable perturbations of the form

$$\delta\hat{n}_{\mathbf{m}} = \tilde{n}^{\mathbf{m}}(x)e^{i[k_m y - k_n^{\parallel} z - \omega_{\mathbf{m}} t]} + c.c., \tag{8}$$

$$\delta\hat{\phi}_{\mathbf{m}} = \tilde{\varphi}^{\mathbf{m}}(x)e^{i[k_m y - k_n^{\parallel} z - \omega_{\mathbf{m}} t]} + c.c., \tag{9}$$

$$\omega_{\mathbf{m}} = \omega_{\mathbf{m}}^r + i\gamma_{\mathbf{m}}, \quad \gamma_{\mathbf{m}} > 0,$$

where we used the symbol $\mathbf{m} = (m,n,l)$ to represent a specific mode, with m, n, and l, respectively, being the azimuthal, axial, and radial mode numbers. k_m and $k_n^{\parallel}$ are, respectively, the azimuthal and the axial non-dimensional wave numbers

$$k_m = 2\pi m\rho_s/L_y, \quad k_n^{\parallel} = 2\pi n\rho_s/L_z. \tag{10}$$

We assume that in the reference frame of interest, the flow velocity has a zero radial average (at $t=0$)

$$\langle V_0\rangle_x = \int_0^{L_x} V_0(x)dx = 0. \tag{11}$$

The above relation is a simplifying assumption. The ZF can have a net rotation in the lab frame, as a result of its interaction with the wall (see Ref. 28). Therefore, if one enforces the boundary conditions on the flow, Eq. (11) must be relaxed. Linear solutions of a system with nonzero radial average $(x',y',z';t')$ and $dy'/dt' = \langle V_0'\rangle_x \neq 0$, which satisfy Eqs. (5) and (6), or equivalently the linear eigenvalue equation (62), are identical to the solutions of the system with zero radial average $\langle V_0\rangle_x = 0$, except for a Doppler shift in frequency $(\omega_{\mathbf{m}}^r = \omega_{\mathbf{m}}^{lr} - \langle V_0'\rangle_x/k_m)$. Moreover, the quasilinear fluxes of these two systems (differing by a net azimuthal flow velocity of $\langle V_0'\rangle_x$) are identical, as can be seen from the relations for the turbulent particle and vorticity fluxes, respectively, in Eqs. (22) and (39).

III. TURBULENT FLUXES

A. Quasilinear particle flux

For the mode $\mathbf{m}$, the (non-dimensional) quasilinear turbulent particle flux $\Gamma_{\mathbf{m}}$ is given by

$$\Gamma_{\mathbf{m}} = \langle\delta\hat{v}_x^{\mathbf{m}}\delta\hat{n}^{\mathbf{m}}\rangle, \tag{12}$$

where we represent the averaging over the directions of symmetry y and z as

$$\langle\ \ \rangle = \frac{1}{L_yL_z}\int_0^{L_y}dy\int_0^{L_z}dz. \tag{13}$$

In order to calculate $\Gamma_{\mathbf{m}}$, using Eqs. (8) and (9), we obtain $\tilde{n}_{\mathbf{m}}$ from the linear continuity Eq. (6)

$$\tilde{n}_{\mathbf{m}} = \frac{-k_m v_d(x) - i\alpha_n}{k_m V_0(x) - \omega_{\mathbf{m}} - i\alpha_n}\tilde{\varphi}_{\mathbf{m}}, \tag{14}$$

where we used $\delta\hat{v}_x = -\partial_y\delta\hat{\phi}$ and we defined the parallel diffusion rate as

$$\alpha_n = (k_n^{\parallel})^2 D_\parallel. \tag{15}$$

Now, $\Gamma_{\mathbf{m}}$ is given by

$$\begin{aligned}\Gamma_{\mathbf{m}} &= \langle\delta\hat{n}_{\mathbf{m}}\delta\hat{v}_x^{\mathbf{m}}\rangle \\ &= \tilde{n}_{\mathbf{m}}\left(\tilde{v}_x^{\mathbf{m}}\right)^* + c.c. = 2\mathrm{Re}\left[ik_m\tilde{\varphi}_{\mathbf{m}}^*\tilde{n}_{\mathbf{m}}\right] \\ &= 2\mathrm{Re}\left[\frac{-ik_m^2 v_d(x) + k_m\alpha_n}{k_m V_0(x) - \omega_{\mathbf{m}} - i\alpha_n}\right]|\tilde{\varphi}_{\mathbf{m}}|^2 \\ &= \frac{v_d(x)[\gamma_{\mathbf{m}} + \alpha_n] + \alpha_n\left(V_0(x) - \omega_{\mathbf{m}}^r/k_m\right)}{|V_0(x) - \omega_{\mathbf{m}}/k_m - i\alpha_n/k_m|^2}\langle\delta\hat{\phi}_{\mathbf{m}}^2\rangle,\end{aligned} \tag{16}$$

where we used $\langle\delta\hat{\phi}_{\mathbf{m}}^2\rangle = 2|\tilde{\varphi}_{\mathbf{m}}^2|$. Equation (16) can be written in terms of a diffusion flux, which is proportional to the local value of the density gradient $dn_0(x)/dx$, and a convective pinch term

$$n_0(x)\Gamma_{\mathbf{m}} = -\mathrm{D}_{\mathbf{m}}(x)\frac{d}{dx}n_0(x) + V^{\mathrm{pinch}}_{\mathbf{m}}(x)n_0(x), \tag{17}$$

$$\mathrm{D}_{\mathbf{m}}(x) = \frac{\gamma_{\mathbf{m}} + \alpha_n}{|V_0(x) - \omega_{\mathbf{m}}/k_m - i\alpha_n/k_m|^2}\langle\delta\hat{\phi}^2_{\mathbf{m}}\rangle, \tag{18}$$

$$V^{\mathrm{pinch}}_{\mathbf{m}}(x) = \frac{\alpha_n\left(V_0(x) - \omega^r_{\mathbf{m}}/k_m\right)}{|V_0(x) - \omega_{\mathbf{m}}/k_m - i\alpha_n/k_m|^2}\langle\delta\hat{\phi}^2_{\mathbf{m}}\rangle. \tag{19}$$

Since $\gamma_{\mathbf{m}} > 0$ (as defined in Eq. (10)), the diffusion coefficient defined in Eq. (18) is positive-definite. Thus, for a monotonically decreasing density (i.e., $dn_0/dx < 0$), the diffusive particle flux is always in the outward direction. On the other hand, the convective pinch term can be in the inward or outward direction, depending on the structure of the flow. We obtain the total particle flux resulting from all the modes present in a turbulent system by summing over all the azimuthal (m) and axial (n) and radial (l) mode numbers

$$\Gamma = \sum_{\mathbf{m}} n_0(x)\Gamma_{\mathbf{m}}, \tag{20}$$

where we used the following notation

$$\sum_{\mathbf{m}} = \sum_{m=-\infty}^{\infty}\sum_{n=-\infty}^{\infty}\sum_{l=1}^{\infty}. \tag{21}$$

The total particle flux Γ is obtained by summing over all the modes

$$\Gamma = n_0\sum_{\mathbf{m}}\alpha_n\frac{[1+\gamma_{\mathbf{m}}/\alpha_n]v_d(x) + V_0(x) - \omega^r_{\mathbf{m}}/k_m}{|V_0(x) - \omega_{\mathbf{m}}/k_m - i\alpha_n/k_m|^2}\langle\delta\hat{\phi}^2_{\mathbf{m}}\rangle. \tag{22}$$

The above relation can be written in terms of diffusion and convection fluxes as

$$\Gamma = -\mathrm{D}_\Gamma(x)\frac{d}{dx}n_0(x) + V^{\mathrm{pinch}}(x)n_0(x), \tag{23}$$

$$\mathrm{D}_\Gamma(x) = \sum_{\mathbf{m}}\mathrm{D}_{\mathbf{m}}(x), \quad V^{\mathrm{pinch}}(x) = \sum_{\mathbf{m}}V^{\mathrm{pinch}}_{\mathbf{m}}(x). \tag{24}$$

In Equation (22), the real and imaginary part of $\omega_{\mathbf{m}}$, and the functional form of $\delta\varphi_{\mathbf{m}}$ are determined from the linear eigenvalue equation Eq. (62).

In the expression for particle flux Γ given by Eq. (22), the numerator of the argument of the sum has the form of a competition between the local drift-diffusion relaxation rate $\omega^*(x) = k_m v_d(x)$, which for $v_d > 0$ results in the diffusive outward particle flux, and the local rate of pumping by waves $\omega^r_{\mathbf{m}} - V_0(x)/k_m$, which is the mode frequency Doppler shifted by the flow velocity. From the particle flux relation in Eq. (22), we observe that for mode $\mathbf{m}$, a net inward flux can be driven if the following condition is satisfied:

$$\omega^r_{\mathbf{m}} > k_m V_0(x) + k_m v_d(x)\left[1 + \frac{\gamma_{\mathbf{m}}}{\alpha_n}\right]. \tag{25}$$

The right hand side of the inequality is explicitly dependent on the flow profile $V_0(x)$ and drift velocity profile $v_d(x)$. Moreover, the values of the eigenfrequency $\omega^r_{\mathbf{m}}$ and growth rate $\gamma_{\mathbf{m}}$ are implicitly dependent on the flow structure and magnitude, as it can be seen from the linear eigenvalue equation (62). From the condition given by Eq. (25), we observe that the flow shear can strengthen the anti-relaxation pumping at some radii, while weakening the pumping at other radii. For strong enough flow shear, flow-enhanced pumping can defeat the relaxation, which will result in a net inward flux of particles. The physical mechanism through which the flow can cause the resistive drift waves to carry the particle flux in the inward (up-gradient) direction is the flow enhanced pumping (or the Doppler effect).

Observation of local inward particle flux was reported in Ref. 54 in the direct numerical simulation of HW turbulence using an implicit relaxation technique and allowing for nonlocality. Although direct comparison of the results in Ref. 54 to our quasilinear theory is only applicable to the limited case of weak turbulence regime, both our theory and Ref. 54 share the belief that inward fluxes in the HW system are the result of nonlocal effects, which in our theory is manifested in the form of global pumping rate given by the drift wave (DW) frequency. However, in Ref. 54, the relation to ZF shearing and its effect on the particle flux have not been discussed or analyzed. The authors have related their observed inward flux to large scale eddies with scales comparable to background scale-length. This begs the question whether the inward flux was driven by the flow shear. Moreover, the mechanism by which the turbulence is responsible for this inward flux has not been determined. In our quasilinear model, only the drift-KH modes with $k_\parallel \neq 0$ can be responsible for driving this inward flux. However, in a fully nonlinear simulation like in Ref. 54, it would be interesting to see if nonlinear mechanisms such as generalized KH[52] can drive an inward flux of particles as well.

In order to better understand Eq. (25), we study two different cases: First is the classic drift waves example in which $V_0 \approx 0$. In the next case, v_d is uniform and only the flow shear can result in an inward flux. For the classical example of resistive drift wave turbulence ($V_0 \approx 0$), the turbulent particle flux from drift resistive waves for an arbitrary value of α_n (assuming $\omega^r_{\mathbf{m}} \gg \gamma_{\mathbf{m}}$) is given by

$$\Gamma = n_0\sum_{\mathbf{m}}\alpha_n\frac{v_d(x) - \omega^r_{\mathbf{m}}/k_m}{|\omega_{\mathbf{m}}/k_m - i\alpha_n/k_m|^2}\langle\delta\hat{\phi}^2_{\mathbf{m}}\rangle, \quad V_0 \approx 0. \tag{26}$$

The outward particle flux is due to relaxation of the density gradient (diffusion), and the inward flux (working as anti-relaxation) is due to the pumping by waves. Since drift waves are global modes, this pumping rate is constant at all radii. For a non-uniform v_d, the relaxation rate $\omega^*(x) = k_m v_d$ can be locally smaller than $\omega^r_{\mathbf{m}}$, which results in driving a flux of particles in the inward, up-gradient direction. The parameter range of interest is the near-adiabatic regime in which the parallel diffusion timescale is the smallest characteristic time scale of the system: $\alpha_n \gg \omega_{\mathbf{m}}, k_m V_0$. In this regime, the drift wave frequency in the absence of flow shear and for a uniform v_d is obtained from the linear dispersion relation as

$$\omega^{0,r}_{\mathbf{m}} = \frac{v_d k_m}{1 + k^2_\perp}, \tag{27}$$

where $k_\perp^2 = -\nabla_\perp^2 \hat{\phi}/\hat{\phi}$. Substituting from Eq. (27) in Eq. (26), the local particle flux for uniform v_d is given by

$$\Gamma = -D_\Gamma \frac{dn_0}{dx} > 0, \quad \text{for constant } v_d \text{ and } V_0 \approx 0, \tag{28}$$

$$D_\Gamma = \sum_{\mathbf{m}} \frac{k_\perp^2}{1+k_\perp^2} \frac{k_m^2}{\alpha_n} \langle \delta\hat{\phi}_{\mathbf{m}}^2 \rangle > 0. \tag{29}$$

Thus, for a uniform v_d and in the absence of flow shear, the net turbulent particle flux resulting from the resistive drift waves is always outward. This is due to the fact that the finite Larmor radius (FLR) correction of polarization current compressibility reduces the mode frequencies (denominator of the fraction on the right hand side of Eq. (27)), and consequently at all radii $\omega^* > \omega_{\mathbf{m}}^r$.

Now, we consider a system with uniform v_d but with a finite amplitude non-uniform flow $V_0(x)$. With the assumption of a uniform v_d, from Eq. (66), the mode frequency $\omega_{\mathbf{m}}$ has the following functional form:

$$\omega_{\mathbf{m}}^r = k_m v_d \, c\left(\frac{V_0^{\max}}{v_d}, \rho^*\right). \tag{30}$$

In the limit where $V_0^{\max}/v_d \to 0$, $\omega_{\mathbf{m}}^r$ is linearly proportional to v_d and is given by the classical electron drift wave frequency given by Eq. (27). We define the change in the mode frequency due to the presence of the flow as $\Delta\omega_{\mathbf{m}}^r$

$$\Delta\omega_{\mathbf{m}}^r = \omega_{\mathbf{m}}^r - \omega_{\mathbf{m}}^{r,0}. \tag{31}$$

$\Delta\omega_{\mathbf{m}}^r$ does not contain a linear v_d dependence, and in the limit of $V_0^{\max}/v_d \to 0$, we have $\Delta\omega_{\mathbf{m}}^r \to 0$. Therefore, we can write the particle flux in the adiabatic regime as

$$\Gamma = -D_\Gamma \frac{dn_0}{dx} + \bar{V} n_0, \tag{32}$$

$$\bar{V} = \sum_{\mathbf{m}} \frac{k_m^2}{\alpha_n} \left(V_0(x) - \Delta\omega_{\mathbf{m}}^r/k_m\right) \langle \delta\hat{\phi}_{\mathbf{m}}^2 \rangle. \tag{33}$$

In Eq. (32), the first term on the right hand side is the diffusive flux with the diffusion coefficient D_Γ given in Eq. (29). The second term is the convective pinch flux with the effective pinch velocity $\bar{V}$ given in Eq. (33). $\bar{V}$ can only be non-zero because of the presence of flow velocity $V_0(x)$. In the limit of $V_0^{\max} \to 0$, since $\bar{V} \to 0$, we recover the result in Eq. (28) for particle flux from drift resistive waves in the adiabatic regime.

Hydrodynamic limit: In the pure hydrodynamic limit for which $\alpha_n/k_m \ll V_0, \omega_{\mathbf{m}}/k_m$, continuity and vorticity equations decouple and the electric potential ϕ is the active variable determining the dynamics of the system. Solutions to the familiar Rayleigh's eigenvalue equation (which is introduced later in Eq. (63)) will determine the linear eigenfunctions, frequencies, and growth rates. In this limit, the particle flux relation in Eq. (22) can be written as a diffusion flux

$$\Gamma \approx -D_\Gamma \frac{dn_0}{dx},$$
$$D_\Gamma = \sum_{\mathbf{m}} \frac{\gamma_{\mathbf{m}}}{|V_0(x) - \omega_{\mathbf{m}}^r/k_m|^2} \langle \delta\hat{\phi}_{\mathbf{m}}^2 \rangle. \tag{34}$$

Note that in the above relation, $\gamma_{\mathbf{m}}$ is defined as positive definite in Eq. (10). Thus, in the hydrodynamic limit for a monotonically decreasing density profile ($dn_0/dx < 0$), the particle flux is always diffusively driven in the outward direction: $\Gamma > 0$. The pure KH modes ($k_\parallel = 0$) for which $\alpha_n = 0$ are also in the hydrodynamic regime, and as a result, the quasilinear particle flux of the pure KH modes is strictly outward.

Flat density profile regime ($\nabla n_0 = 0$): From Eqs. (17) through (19), we can see that in the case of a flat density profile, non-zero turbulent particle flux can only come from the convective pinch term with $\alpha_n \neq 0$. In the regime where initially $\nabla n_0 = 0$, flow shear (∇V_0) is the only source of free energy which can drive an instability and a turbulent particle flux.

We can perform the Rayleigh stability analysis for these modes on the linear eigenvalue equation with $v_d = 0$

$$\left(\partial_x^2 - k_m^2\right)\delta\hat{\phi} - \frac{k_m V_0''(x)}{k_m V_0 - \omega}\delta\hat{\phi} + i\alpha_n \left[\frac{k_m V_0(x) - \omega}{k_m V_0(x) - i\alpha_n - \omega}\right]\delta\hat{\phi} = 0. \tag{35}$$

Multiplying the above equation by $\delta\hat{\phi}^*$, integrating over x, and taking the imaginary part of the equation, we obtain the following condition for the instability:

$$\omega_i = \frac{\alpha_n \int \frac{k_m V_0 - \omega_r}{|k_m V_0 - i\alpha_n - \omega|^2} |\delta\hat{\phi}|^2 dx}{\int \frac{k_m V_0''}{|k_m V_0 - \omega|^2} |\delta\hat{\phi}|^2 dx} > 0. \tag{36}$$

The above relation is the instability condition for these *resistive-KH* modes, which is a generalized form of the Rayleigh's inflection point criterion for the pure KH modes. Eq. (36) implies that unlike the pure KH modes, which are also only driven by the flow shear, existence of an inflection point in the flow profile is not a necessary condition for the instability of these modes. Turbulent particle flux in this limit can be obtained from Eq. (32) by setting $dn_0/dx = 0$. Thus, the direction of the particle flux can be either inward or outward, depending on the flow structure.

B. Quasilinear turbulent vorticity flux

For the mode $\mathbf{m}$, the quasilinear turbulent vorticity flux $\Pi_{\mathbf{m}}$ is given by

$$\Pi_{\mathbf{m}} = \langle \delta\hat{v}_x^{\mathbf{m}} \nabla^2 \delta\hat{\phi}_{\mathbf{m}} \rangle. \tag{37}$$

Total vorticity flux is obtained by summing over all the mode numbers

$$\Pi = \sum_{\mathbf{m}} \Pi_{\mathbf{m}}. \tag{38}$$

We obtain the total vorticity flux from substituting Eq. (14) in the vorticity equation (i.e., Eq. (5)), multiplying by $\delta\hat{v}_{\mathbf{m}}$, averaging over y and z, and summing over all mode numbers

$$\Pi = \sum_{\mathbf{m}} \left\{ \frac{\gamma_{\mathbf{m}} v_d(x) + \alpha_n \left(v_d(x) + V_0(x) - \omega^r_{\mathbf{m}}/k_m \right)}{\left| k_m V_0(x) - \omega_{\mathbf{m}} - i\alpha_n \right|^2} - \gamma_{\mathbf{m}} \frac{v_d(x) + V''_0(x)}{\left| k_m V_0(x) - \omega_{\mathbf{m}} \right|^2} \right\} \langle \left(\delta\hat{v}^{\mathbf{m}}_x \right)^2 \rangle.$$

The above relation can alternatively be written as

$$\Pi = \Pi^R - \chi_y V''_0, \tag{39}$$

$$\chi_y = \sum_{\mathbf{m}} \frac{\gamma_{\mathbf{m}} \langle \delta\hat{\phi}^2_{\mathbf{m}} \rangle}{\left| V_0(x) - \omega_{\mathbf{m}}/k_m \right|^2}, \tag{40}$$

$$\Pi^R = \sum_{\mathbf{m}} \frac{\gamma_{\mathbf{m}} v_d(x) + \alpha_n \left(v_d(x) + V_0(x) - \omega^r_{\mathbf{m}}/k_m \right)}{\left| V_0(x) - \omega_{\mathbf{m}}/k_m - i\alpha_n/k_m \right|^2} \times \langle \delta\hat{\phi}^2_{\mathbf{m}} \rangle - \chi_y v_d. \tag{41}$$

Here, we define χ_y in the second term in Eq. (39) as the turbulent viscosity, which directly relates the flow vorticity gradient to the turbulent vorticity flux. The turbulent viscosity term can be rewritten to obtain a proper flow velocity diffusion form (divergence of a flux) as

$$-\chi_y V''_0 = -\partial_x [\chi_y V'_0] + \chi'_y V'_0. \tag{42}$$

On the right hand side of the above equation, the first term is the turbulent viscous diffusion of flow velocity and the second term is a flow advection term with $V_{\text{adv}} = \chi'_y$. When V_0 and V''_0 are both zero, only the first term in Eq. (39) can result in a non-zero turbulent vorticity flux. In analogy with Ref. 27, we call this term the residual vorticity flux.

Vorticity flux for the pure KH modes ($k_\parallel = 0$) is obtained by setting $\alpha = 0$, which gives

$$\Pi = -\chi_y V''_0, \quad k_\parallel = 0, \tag{43}$$

where χ_y is given by Eq. (40). Although the residual vorticity of the pure KH modes is zero and density gradient cannot drive these instabilities, in the regime which these modes unstable, they relax the $E \times B$ flow profile via turbulent viscous diffusion.[55,56] The Reynolds stress for these instabilities has been shown to be proportional to the tilting angle of the axis of vortices with respect to the direction of the flow.[55] Using Eq. (22), the residual vorticity flux can be simply written as

$$\Pi^R = \frac{\Gamma}{n_0} - \chi_y v_d. \tag{44}$$

Through Π^R, the density gradient ∇n_0 drives a stress on the flow. In the adiabatic regime for which $\alpha_n \gg \omega$, the particle flux dependent term of the residual vorticity behaves as $\frac{\Gamma}{n_0} \propto 1/\alpha_n$ and is therefore negligible comparing to the second term on the right hand side of Eq. (44). Hence, the Γ dependent term in Π^R results from non-adiabaticity of the electrons. For large flows, from Eq. (41), we can see that the residual vorticity is also a function of the flow. Had the flow been constant as a function of radius x, this functional dependence would have been merely a trivial reference frame effect. However, the dependence on x means that it is actually the flow gradients which are at work in driving the turbulent vorticity flux and can exert stress on the flow itself, resulting in the self-reorganization of the flow. The equation for the time evolution of the ZF is given by

$$\partial_t V_0 = -\partial_x \langle \delta\hat{v}_x \delta\hat{v}_y \rangle - \gamma_d V_0, \tag{45}$$

where the first term on the right hand side is the Reynolds force and the second term is a drag force due to the collisions with neutrals. Using Eqs. (39) to (44) and the Taylor identity

$$\langle \delta\hat{v}_x \nabla^2 \delta\hat{\phi} \rangle = \partial_x \langle \delta\hat{v}_x \delta\hat{v}_y \rangle, \tag{46}$$

we can write Eq. (45) as

$$\left[\partial_t + \chi'_y \partial_x \right] V_0 = \chi_y v_d - \frac{\Gamma}{n_0} + \partial_x \left[\chi_y \partial_x V_0 \right] - \gamma_d V_0. \tag{47}$$

In the above equation, the second term on the left hand side is a turbulent advection of the flow velocity, with the advection velocity given by χ'_y. The first term on the right hand side, which comes from residual vorticity Π^R, is positive definite for $v_d > 0$ and drives a force on the flow in the direction of electron diamagnetic velocity, i.e., positive y direction. The second term on the right hand side, which also comes from the residual vorticity, can drive a force on the flow in the positive or negative y direction, depending on the sign of the particle flux. The third term on the right hand side is the turbulent viscous diffusion of the flow velocity with turbulent viscosity given by χ_y, which acts to relax the flow shear. We can also write the residual vorticity drive of the ZF in terms of the density diffusion and convection terms, using Eq. (23) for Γ

$$[\partial_t + \chi'_y \partial_x] V_0 = (\chi_y - D_\Gamma) v_d - V_{\text{pinch}} + \partial_x [\chi_y \partial_x V_0] - \gamma_d V_0, \tag{48}$$

where D_Γ is the particle diffusion coefficient (defined in Eqs. (18) and (23)), and V_{pinch} is the pinch velocity of the turbulent particle flux (defined in Eqs. (19) and (23)). We can furthermore obtain the evolution equation for the flow vorticity V'_0 by taking a partial derivative of Eq. (45) with respect to x, which results in

$$\partial_t V'_0 = \partial_x \left[\chi_y v_d - \frac{\Gamma}{n_0} \right] + \partial_x \left[\chi_y \partial_x V'_0 \right] - (\gamma_d V_0)'. \tag{49}$$

IV. QUASILINEAR POTENTIAL ENSTROPHY CONSTRAINT

The modified Hasegawa-Wakatani system of Equations (5) and (6) has two classes of fluxes, turbulent particle flux and turbulent vorticity flux, which we obtained, respectively, in Eqs. (22) and (39). Here, we determine an overall constraint on the relaxation in the form of a relation between these two classes of flux and the two sources of free energy, which is required by positive definite turbulence enstrophy

production. In order to obtain this relation, first we subtract Eq. (5) from Eq. (6) and obtain

$$(\partial_t + V_0\partial_y)(\delta\hat{n} - \nabla^2\delta\hat{\phi}) - \delta\hat{v}_x(v_d + \partial_x^2 V_0) = 0. \quad (50)$$

The above relation is the linearized form of the conservation relation for the total potential vorticity $q = q_0 + \delta q$

$$\frac{d}{dt}q = 0, \quad q = \ln n - \nabla^2\hat{\phi}, \quad (51)$$

$$q_0 = \ln n_0(x) - V_0'(x), \quad (52)$$

$$\delta q = \delta\hat{n} - \nabla^2\delta\hat{\phi}. \quad (53)$$

Now, we multiply Eq. (50) by $\delta\hat{n} - \nabla^2\delta\hat{\phi}$ and average over the directions of symmetry (y and z) to obtain

$$\frac{\partial}{\partial t}\frac{\langle\delta q_{\mathbf{m}}^2\rangle}{2} = (\Gamma_{\mathbf{m}} - \Pi_{\mathbf{m}})(v_d + V_0'') > 0. \quad (54)$$

Equation (54) is the condition for the (positive definite) growth of potential enstrophy of the fluctuations. On the right hand side of Eq. (54), the sign of the difference between the turbulent fluxes of particle and vorticity $(\Gamma_{\mathbf{m}} - \Pi_{\mathbf{m}})$ is locally (at any radial location) bound to the free energy sources of density and vorticity gradient. According to the condition (54), at a radial location x where $(v_d(x) + V_0''(x)) > 0$, if the direction of the turbulent particle flux is inward $(\Gamma_{\mathbf{m}} < 0)$, then vorticity flux must be also in the inward direction $\Pi_{\mathbf{m}} < 0$ and its amplitude larger than $\Gamma_{\mathbf{m}}$. Here, we remind the reader that the turbulent vorticity flux $\Pi_{\mathbf{m}}$ is related to Reynolds stress $\Pi_{\mathbf{m}} = \langle\delta\hat{v}_x^{\mathbf{m}}\delta\hat{v}_y^{\mathbf{m}}\rangle$ via the Taylor Identity Eq. (46). Moreover, we can multiply Eq. (50) by $\delta\hat{v}_x^{\mathbf{m}}$ and average over the symmetric dimensions to obtain the PV flux as

$$\langle\delta\hat{v}_x^{\mathbf{m}}\delta q_{\mathbf{m}}\rangle = \Gamma_{\mathbf{m}} - \Pi_{\mathbf{m}} = \gamma_{\mathbf{m}}\frac{\langle(\delta\hat{v}_x^{\mathbf{m}})^2\rangle}{|k_m V_0 - \omega_{\mathbf{m}}|^2}(v_d + V_0''). \quad (55)$$

Since $\gamma_{\mathbf{m}}$ is defined as positive definite in Eq. (10), the above relation puts the same sign constraint between $\Gamma_{\mathbf{m}} - \Pi_{\mathbf{m}}$ and $v_d + V_0''$ as Eq. (54) did. Moreover, by eliminating $\Gamma_{\mathbf{m}} - \Pi_{\mathbf{m}}$ from Eqs. (54) and (55), we obtain

$$\frac{\partial}{\partial t}\langle\delta q_{\mathbf{m}}^2\rangle = \langle(\delta\hat{v}_x^{\mathbf{m}})^2\rangle\frac{\gamma_{\mathbf{m}}(v_d + V_0'')^2}{|k_m V_0 - \omega_{\mathbf{m}}|^2}. \quad (56)$$

For a near marginal stability mode $(\omega_{\mathbf{m}}^r \gg \gamma_{\mathbf{m}})$, the above equation can be expanded to obtain

$$\begin{aligned}\frac{\partial}{\partial t}\langle\delta q_{\mathbf{m}}^2\rangle &= \lim_{\gamma_{\mathbf{m}}\to 0}\langle(\delta\hat{v}_x^{\mathbf{m}})^2\rangle\frac{\gamma_{\mathbf{m}}(v_d + V_0'')^2}{(k_m V_0 - \omega_{\mathbf{m}}^r)^2 + (\gamma_{\mathbf{m}})^2},\\ &= \pi k_m\delta(V_0 - \omega_{\mathbf{m}}^r/k_m)(v_d + V_0'')^2\langle\delta\hat{\phi}_{\mathbf{m}}^2\rangle,\\ &= \pi k_m\sum_j\delta(x - x_{c,j})\frac{(v_d + V_0'')^2}{|V_0'|}\langle\delta\hat{\phi}_{\mathbf{m}}^2\rangle,\\ V_0(x_c) &= \omega_{\mathbf{m}}^r/k_m. \end{aligned} \quad (57)$$

The functional form of Eq. (57) implies that the interaction between a near marginal mode and the ZF is in the form of a resonant interaction at the critical radii x_c, for which the flow velocity is equal to the wave phase velocity.

Equations (54)–(56) were obtained based on the assumption that the spatial length scale for the variation of the background density is large (of the order L_x) compared to the flow and turbulence. For the general case, taking full account of the spatial variation of the background density, we have derived the equivalent relations (A13), (A15), and (A16), in the Appendix.

We examine the Equations (54)–(56) for the special case of the adiabatic regime $\alpha_n/\omega \gg 1$, for which $\delta n/n_0 \approx \delta\hat{\phi}$. From Eq. (62), the linear eigenvalue equation to the zeroth order in $\omega/\alpha_n \ll 1$ is given by

$$[k_m V_0 - \omega](\partial_x^2 - k_m^2 - 1)\delta\hat{\phi} - k_m[V_0''(x) + v_d(x)]\delta\hat{\phi} = 0. \quad (58)$$

Performing Rayleigh's inflection point analysis, we find that a necessary condition for instability is that there must exists a point $\bar{x}$ such that

$$V_0''(\bar{x}) + v_d(\bar{x}) = 0. \quad (59)$$

This result is identical to the necessary condition for the inviscid instability of a barotropic flow, in the quasi-geostrophic system, which states that the gradient of the absolute vorticity must change sign somewhere in the flow.[57] Moreover, from Equations (55) and (59), we see that at the point $\bar{x}$, particle and vorticity fluxes balance

$$\Gamma_{\mathbf{m}}(\bar{x}) = \Pi_{\mathbf{m}}(\bar{x}). \quad (60)$$

Consequently, as can be seen from Eq. (54), there is no potential enstrophy production at $\bar{x}$

$$\frac{\partial}{\partial t}\langle\delta q_{\mathbf{m}}^2\rangle(\bar{x}) = 0. \quad (61)$$

V. LINEAR STABILITY AND TURBULENCE PRODUCTION

A. Eigenvalue equation

Eigenfrequencies and eigenfunctions are obtained by solving the linear eigenvalue equation, obtained from substituting (6) in (5):

$$[k_m V_0 - \omega](\partial_x^2 - k_m^2)\delta\hat{\phi} - \left(k_m V_0''(x) - i\alpha_n\left[\frac{k_m V_0(x) + k_m v_d - \omega}{k_m V_0(x) - i\alpha_n - \omega}\right]\right)\delta\hat{\phi} = 0. \quad (62)$$

In the pure hydrodynamic limit $\alpha_n/\omega \to 0$, the eigenvalue relation (62) turns into the Rayleigh's eigenvalue equation

$$[k_m V_0 - \omega](\partial_x^2 - k_m^2)\delta\hat{\phi} - k_m V_0''(x)\delta\hat{\phi} = 0. \quad (63)$$

Solving the Rayleigh's eigenvalue equation gives the eigenfunctions, growth rates, and frequencies. Unstable solutions

of the above equation are Kelvin-Helmholtz modes, which are driven by the flow shear. The pure KH modes ($k_n^{\|}=0$) are a subset of these solutions. A necessary condition for the existence of the KH modes is the presence of an inflection point in the flow profile

$$V''_0(\bar{x})=0. \tag{64}$$

Density perturbation is passively calculated from the continuity equation and is given by

$$\tilde{n}_{\mathbf{m}}=\frac{k_m v_d(x)}{\omega_{\mathbf{m}}-k_m V_0(x)}\tilde{\varphi}_{\mathbf{m}}. \tag{65}$$

We further simplify the linear eigenvalue equation (62) by assuming a uniform drift velocity and eliminating v_d. As a result, we rewrite Eq. (62) as

$$[U-c](\partial_x^2-k_m^2)\delta\hat{\phi}-\left(U''(x)-i\frac{Q_n}{k_m\hat{L}_x}\times\left[\frac{U(x)+1-c}{U(x)-iQ_n/k_m\hat{L}_x-c}\right]\right)\delta\hat{\phi}=0, \tag{66}$$

where we have defined

$$c=\frac{\omega}{k_m v_d},\quad U(x)=\frac{V_0(x)}{v_d},\quad Q_n=\frac{\alpha_n}{v_d/\hat{L}_x},\quad \hat{L}_x=\frac{1}{\rho*}=\frac{L_x}{\rho_s}. \tag{67}$$

For the drift-KH modes with phase velocities comparable to v_d, $Q_n/k_m\hat{L}_x=\alpha_n/k_m v_d$ can be considered as the adiabaticity parameter. Obviously, solutions of the above equation depend on the structure of the scaled flow profile $U(x)$. The unitless parameters which determine the solutions are ρ^*, k_m, Q_n, the amplitude of the flow $U_{\max}=V_0^{\max}/v_d$ (taking the flow structure as invariant and changing the amplitude), and q_x, the wave number describing the spatial variation of the flow profile. We use a standard shooting method to solve Eq. (66) for the complex eigenvlaue c and its related eigenfunction $\delta\hat{\phi}$. We use Dirichlet boundary conditions for simplicity: $\delta\hat{\phi}(0)=\delta\hat{\phi}(L_x)=0$. As a toy model for ZF, we use a sinusoidal profile

$$U(x)=U_{\max}\sin\left[q_x\left(x-\frac{\hat{L}_x}{2}\right)\right], \tag{68}$$

where the non-dimensional wave number given by $q_x=\rho_s/L_{\mathrm{ZF}}$. Spatial scaling of the ZF is in the meso range, which is in accordance with Eq. (4).

Figure 2 shows the ZF profile given by the function $U(\tilde{x})$ with $\rho^*=1/9\approx 0.11$, for $U_{\max}=V_0^{\max}/v_d=1$ and spatial scale of $q_x\hat{L}_x=\pi$. These are parameters which are typical for the CSDX device. This flow profile satisfies the condition Eq. (4)

$$L_{\mathrm{ZF}}=2.86\rho_s\le\sqrt{\rho_s L_x}=3\rho_s. \tag{69}$$

For the CSDX device, since $\rho^*\sim 0.1$ is relatively large, the variation in the spatial scale of ZF is very limited

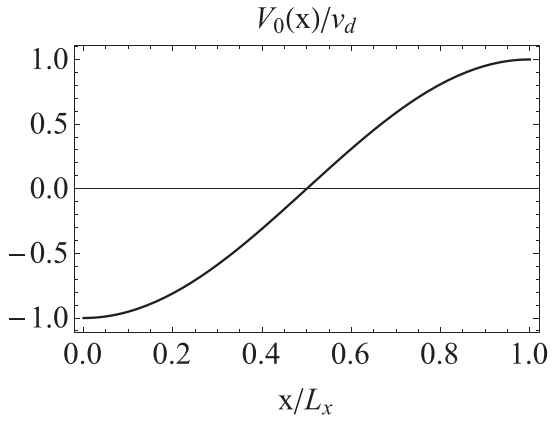

FIG. 2. A toy model for the zonal flow, with $\rho^*=0.11, V_0(\tilde{x})=v_d\sin[q_x(\tilde{x}-\frac{\hat{L}_x}{2})], q_x\hat{L}_x=\pi$.

($\rho_s<L_{\mathrm{ZF}}\le 3\rho_s$). Figure 3(a) shows the growth rate of the first radial eigenmode ($l=1$) as a function of $U_{\max}$ for the ZF with the form given in Fig. 2 and $k_m/q_x=0.3,1,2$. The choice of the first radial eigenmode is due to the convenience of finding this mode as the parameters of the problem change, compared to the higher l numbers. For $k_m/q_x=0.3,1$

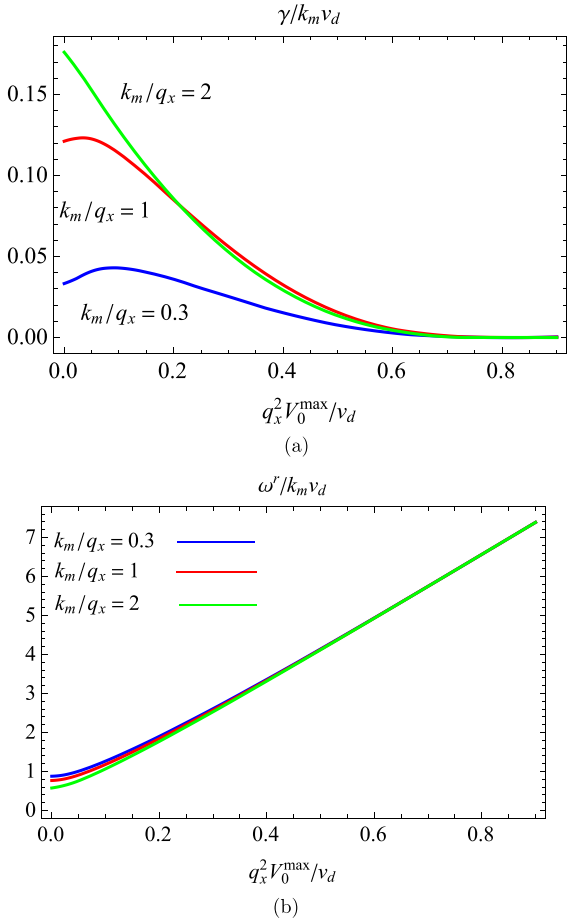

FIG. 3. Growth rate and frequency of ($l=1$), $k_m/q_x=0.3,1,2$ modes as a function of the zonal flow amplitude $V_0^{\max}$ for $\rho^*=0.1, q_x\hat{L}_x=\pi$, and $Q_n=0.3$.

the growth rates increase with the ZF amplitude up to $V_0^{max}/v_d \sim 1$ and to $V_0^{max}/v_d \sim 0.5$, respectively, and after that decreases monotonically. For $k_m/q_x = 2$, the growth rates decrease with the flow amplitude, and the flow always has a destabilizing effect. For all the three values of $k_m\hat{L}_x/q_x = 0.3, 1, 2$, the mode frequency increases with the flow amplitude. Although this increase appears to be of a linear form, changing the sign of the ZF amplitude does not affect the mode frequency or growth rate. As the amplitude of the flow is raised, the growth rate of the mode decreases, and the mode frequency increases. At the critical value for which $U_{\max}^{\text{crit}} = V_0^{\max}/v_d = c_{\text{crit}}$, the growth rate of the mode goes to zero. Substituting c_{crit} in Eq. (66), we obtain the condition for the radial position of the critical layer as

$$U''(c_{\text{crit}}) = -1. \tag{70}$$

As we raise the amplitude of the ZF $U_{\max}$, the above condition will be satisfied at the radial location, for which

$$U_{\max}^{\text{crit}} = q_x^{-2}. \tag{71}$$

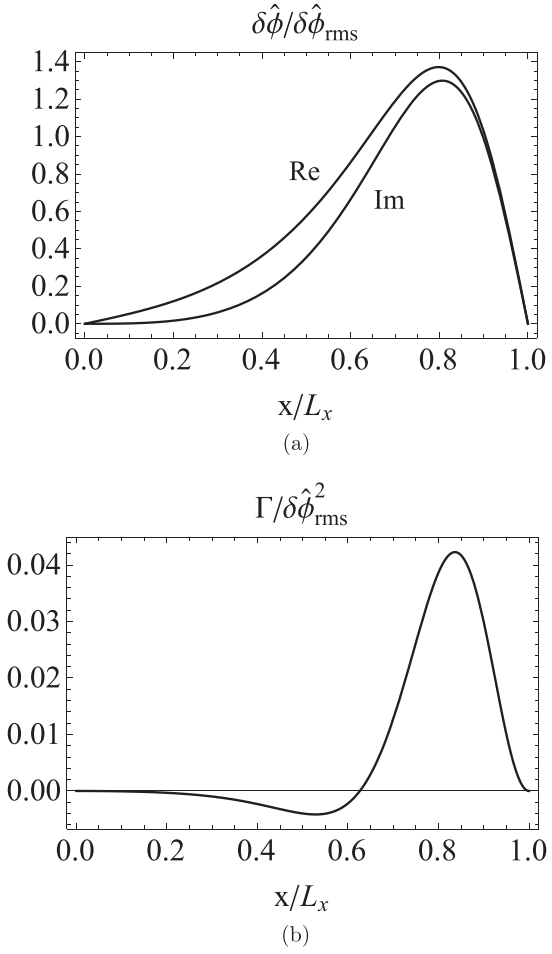

FIG. 4. (a) Real and imaginary part of the first radial eigenmode with eigenfrequency $\omega/k_m v_d = 1.13 + 0.0012i$ for $k_m/q_x = 0.3$, $V_0^{\max}/v_d = 1$, $\rho^* = 0.11$, $q_x\hat{L}_x = \pi$, and $Q_n = 0.3$. (b) Quasilinear particle flux for the $l = 1$ eigenmode depicted in Fig. 4(a), as a function of radial position.

This critical radial location for the profile of Eq. (68) and for $q_x\hat{L}_x = \pi$ is at $x = \hat{L}_x$ and the critical flow amplitude is $U_{\max}^{\text{crit}} = 8.2$. For profiles which are more sheared, i.e., the spatial variation scale of the flow is smaller (or equivalently q_x is larger), the critical amplitude for instability of the flows is lower.

Here, we calculate the quasilinear turbulent flux of particles, using Eq. (16), for our numerically obtained modes. Our goal is to see how big the net inward flux can be, compared to the net outward flux, as a function of the parameters of the system, such as the spatial scales of modes k_m, the spatial scale of ZF q_x, and also the amplitude of the ZF, $V_0^{\max}$.

The real and imaginary parts of the first radial eigenfunction ($l = 1$) is shown in Fig. 4(a) (mode number indices have been dropped), for $k_m/q_x = 0.3, Q_n = 0.3, \rho^* = 0.11$, $q_x\hat{L}_x = \pi$, and $V_0^{\max}/v_d = 1$, and the ZF given by Fig. 2. Since the solutions are linear, the eigenfunction depicted in Fig. 4(a) is normalized to its root mean square value given by

$$\delta\hat{\phi}_{\text{rms}} = \sqrt{\frac{1}{L_x L_y L_z}\int |\delta\hat{\phi}^2| dx dy dz}. \tag{72}$$

In Fig. 4(b), we have plotted the quasilinear particle flux for the eigenmode of Fig. 4(a). The particle flux stagnation points at which $\Gamma(x_{\text{stag}}) = 0$ are given by the solutions of

$$\omega_{\mathbf{m}}^r - k_m V_0(x_{\text{stag}}) - k_m v_d(x_{\text{stag}})\left[1 + \frac{\gamma_{\mathbf{m}}}{\alpha_n}\right] = 0. \tag{73}$$

In Fig. 5, we have plotted the ratio of the radially integrated net inward flux (Γ_{in}) to the radially integrated outward flux (Γ_{out}), as a function of the flow amplitude $V_0^{\max}$, where Γ_{in} and Γ_{out} are given by

$$\begin{aligned} \Gamma_{\text{in}} &= \frac{1}{L_x}\int_0^{L_x} \Gamma\Theta(-\Gamma)dx, \\ \Gamma_{\text{out}} &= \frac{1}{L_x}\int_0^{L_x} \Gamma\Theta(\Gamma)dx. \end{aligned} \tag{74}$$

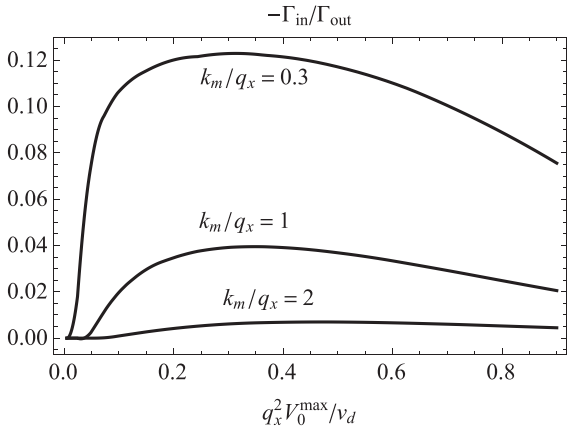

FIG. 5. Ratio of the net inward flux to the net outward flux for the $l = 1$ mode, as a function of the ZF amplitude, for $\rho^* = 0.11$, $q_x\hat{L}_x = \pi$, and $Q_n = 0.3$.

In the above equations, $\Theta(x)$ is the Heaviside step function. In Fig. 5, $q_x\hat{L}_x = \pi$ and $k_m/q_x = 0.3, 1, 2$, and the first radial eigenmode is used ($l = 1$). We can make the following observations in Fig. 5: (i) A minimum exists for the flow amplitude $U^{\mathrm{L}}_{\mathrm{max}}$, below which the flow shear is too small to drive a net inward flux. This minimum value increases with the value of k_m/q_x: for $k_m/q_x = 0.3, 1, 2$, respectively, $q_x^2 U^{\mathrm{L}}_{\mathrm{max}} \approx 0.009, 0.03, 0.08$. (ii) The value of the $-\Gamma_{\mathrm{in}}/\Gamma_{\mathrm{out}}$ decreases with $k_m\hat{L}_x$. This implies that longer wavelength modes (smaller values of k_m/q_x) carry a larger local net inward flux driven by ZF convection.

B. Turbulence energetics

We define $\mathcal{E}(x;t)$, which is the fluctuation energy density averaged over the directions of symmetry

$$\mathcal{E}(x;t) = \frac{1}{2}\langle|\nabla\delta\hat{\phi}|^2 + |\delta\hat{n}|^2\rangle > 0. \tag{75}$$

Evolution of the total wave energy is given by integrating $\mathcal{E}(x;t)$ over the whole volume

$$\frac{\partial}{\partial t}\mathrm{E} = \int \mathcal{E}(x;t)d\tau = \mathrm{P}_{\mathrm{diss}} + \mathrm{P}_n + \mathrm{P}_{\mathrm{ZF}},$$

$$\mathrm{P}_{\mathrm{diss}} = -\int \alpha|\delta\hat{n} - \delta\hat{\phi}|^2 d\tau, \quad \mathrm{P}_n = \int \Gamma v_d(x) d\tau,$$

$$\mathrm{P}_{\mathrm{ZF}} = \int \Pi V_0(x) d\tau,$$

where $d\tau$ is the 3D volume element. The first term on the right hand side is the rate of turbulence energy dissipated due to resistive parallel diffusion, and is negative definite at all x. The second term is the rate of energy released from the density gradient to the turbulence. The third term is the rate of work performed by the flow on the turbulence ($-$Reynolds work). The argument of the last two integral terms can be local sinks or sources, i.e., their signs depend on the sign of their relative fluxes (particle flux or vorticity flux) and the signs of the background velocities (electron diamagnetic drift velocity v_d or flow velocity V_0).

Figure 6 shows the ratio of the rate of energy transferred from the flow to the turbulence (P_{ZF}) to the rate of energy transferred from the density gradient to the turbulence (P_n), as a function of flow amplitude V_0^{max}, for the same parameters as in Fig. 5. P_n is always positive, which means the density gradient always drives the turbulence. For $k_m/q_x = 0.3$, flow transfers energy to turbulence for all flow amplitudes $\mathrm{P}_{\mathrm{ZF}} > 0$. The value of $\mathrm{P}_{\mathrm{ZF}}/\mathrm{P}_n$ remains relatively constant for $V_0^{\mathrm{max}} \gtrsim v_d$. For $k_m/q_x = 1$, flow transfers energy to the turbulence at flow amplitudes lower than a threshold amplitude $q_x^2 V^{\mathrm{max}}/v_d \approx 0.35$, and for flow amplitudes greater than this threshold, turbulence transfers energy to the flow. For $k_m/q_x = 2$, the direction of energy transfer is always from the turbulence to the flow. Therefore, we can see that the direction of the energy transfer changes with the length scale of the modes: for small wave number modes, flow drives the turbulence. As the mode wave number becomes larger compared to the ZF wave number, the direction of energy transfer changes and the modes transfer energy to the flow.

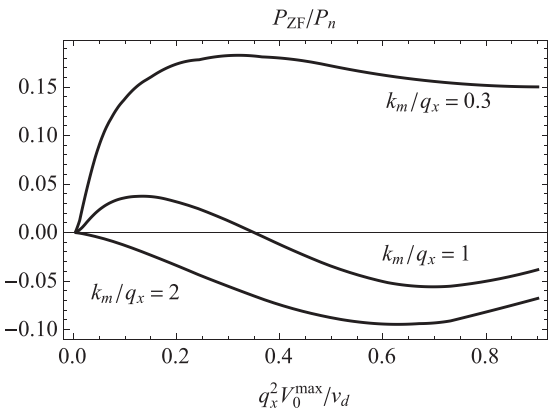

FIG. 6. Ratio of the rate of energy transferred from the flow to the turbulence P_{ZF} to the rate of energy transferred from the density gradient to the turbulence P_{n}, as a function of the flow amplitude V_0^{max}, for the same parameters as in Fig. 5.

In Ref. 12, Zhou *et al.* present experimental evidence of an inward flux on the outer edge of the plasma. The authors suggest that this inward flux is driven, due to the strong flow shear driven at the edge of plasma cylinder through biasing of the edge to amplitudes $V_{E\times B}$ much larger than the electron diamagnetic drift velocity v_d. In comparison, the observation of the inward particle flux reported by Cui *et al.* in Refs. 33 and 34 is for an un-biased system in which the flow is self-generated with amplitudes $V_{E\times B} \leq v_d$. Moreover, Zhou *et al.* present a linear analysis of the frequencies and growth rates of different linear instabilities, which can cause the turbulence, including drift-KH, pure KH, and interchange modes. Comparing to their experimental results, they conclude that since both drift-KH and pure KH frequencies are comparable to the experimentally measured frequencies, then the $E \times B$ both flow shear and density gradient must be both responsible for driving the fluctuations. In the analysis of the energetics of our theory, this corresponds to the case where the spatial scaling of the mode is small comparing to the spatial scaling of the flow shear (e.g., the curve for $k_m/q_x = 0.3$ in Fig. 6), for which both the flow shear and the density gradient drive the turbulence. However, Zhou *et al.* do not say which of these unstable modes is directly responsible for driving the inward flux. Our theoretical model determines these modes to be the $k_\parallel \neq 0$ drift-KH modes and not the $k_\parallel = 0$ pure KH modes.

VI. CONCLUSION AND DISCUSSION

Self-generation of zonal flows has been the subject of many theoretical studies,[27,35] as well as numerical simulation of fluid models,[36,40–44] Some of the interesting aspects of the aforementioned studies are flow formation mechanisms, turbulence regulation and reduction by (zonal) flows, transport of particles, heat and momentum, and the effect of zonal flows on transport. However, there has been little work done on the effect of locally varying fluxes of particles on the reorganization of flow profiles and vice versa. Moreover,

quantitative study of zonal flow generation via residual stress and the comparison to other flow generation mechanisms in the same system have not gotten enough attention.

In this paper, we study the interplay between the transport of particles, vorticity, the background density, and the flow shear, using a simple, modified HW model. More specifically, we show how the competition between the terms contributing to the particle flux, which are functions of the global parameters of the system, and the terms which are dependent on the local values can result in a local inward flux of particles. Moreover, due to the conservation laws of this system, we show that the vorticity flux is linked and constrained to the particle flux through the residual vorticity. As a result, the variation of particle flux can directly change the local value of vorticity flux.

The primary purpose of this paper is to explain the theory, whereas the comparisons of the theory we discussed here to the new experimental results are to be found in Ref. 33 by Cui *et al*. The following is a summary of our results:

(i) We derive the flow dependent quasilinear expression for the particle flux, which consists of a diffusive relaxation flux in the outward direction and a convective pinch, which can be either inward or outward, depending on the zonal flow structure.

(ii) We identify a mechanism for driving an inward particle flux by the zonal flow: Flow enhanced pumping (Doppler effect) by the waves can overcome the outward diffusive relaxation flux, leading to a net inward flux of particles. Moreover, we obtain the condition for driving a net inward flux in Eq. (25). The free energy for driving this up-gradient particle flux comes from flow shear (∇V_0).

(iii) Quasilinear expression for the vorticity flux is obtained. This transport flux consists of a viscous diffusive term and a residual vorticity flux. The latter can drive a flow shear from an initial state of zero flow shear. The functional form of residual vorticity is a sum of a positive definite term directly proportional to ∇n_0, and a term directly proportional to particle flux Γ, which can be locally positive or negative and is driven by both ∇n_0 and the flow shear (through its convective pinch part).

(iv) Using the positive definite enstrophy production, we obtain a constraint relation in Eq. (54), which links the transport of particles and vorticity and also the background gradients.

(v) We obtain the linear eigenvalue equation for this system to study the effect of the flow on the eigenmodes, as well as the quasilinear fluxes resulting from these modes. Assuming a toy zonal flow profile, we observe that the threshold flow amplitude for the instability of the mode is $V_{\max}^{\text{crit}} = v_d L_{\text{ZF}}^2/\rho_s^2$, where L_{ZF} is the characteristic length scale of the zonal flow. As the flow amplitude approaches $V_{\max}^{\text{crit}}$, the mode frequency increases toward $V_{\max}^{\text{crit}} k_y$, and mode growth rate approaches zero.

(vi) Comparing the total inward fluxes to outward fluxes as defined in Eq. (74), we observe that inward particle fluxes of larger magnitude are driven for longer wavelength modes compared to characteristic length scale of the ZF $(k_y < L_{\text{ZF}}^{-1})$. Moreover, for short wavelength modes, there is a threshold flow amplitude below which the inward fluxes does not exist at all.

(vii) While a monotonically decreasing density gradient always performs positive work on the turbulence, flow can (quasilinearly) transfer energy to the turbulence or extract energy from turbulence. We observe that for longer wavelength modes as compared to the characteristic length scale of the ZF $(k_y < L_{\text{ZF}}^{-1})$, the flow drives the turbulence, whereas for $(k_y > L_{\text{ZF}}^{-1})$, the turbulence drives the flow.

(viii) This work is primarily analytical. Despite numerous computer studies of this system, no specific tests of the theory in this paper are available. Thus, we suggest the following tests in a nonlinear numerical simulation of this system:

  (a) Can a $\Gamma < 0$ over a finite region be driven by a self-consistent flow without biasing, given different initial background pressure profiles?

  (b) How does the vorticity gradient for a saturated zonal flow profile scale with $1/L_n \sim \frac{dn}{dx}/n$ and Γ and whether our theory is successful in predicting the saturated vorticity structure (see Eq. (49))?

  (c) Can the theory predict the location of the sign reversal of Γ based on the given background quantities?

Regarding the numerical simulations, there have been extensive studies of HW including flows. While Reynolds stress driven flows and their effect on transport and confinement improvement with shear layer are well known, little has been done on the flow structure and its relation to transport. This point has been amplified in (viii) above, which suggested some numerical tests on theory.

An improvement to the current model is the inclusion of finite ion temperature effects, which we intend to study in our future work. The presence of a finite ion temperature profile affects the stability of pure KH waves, as well as drift-KH waves. Furthermore, introducing the additional source of free energy in the ion temperature gradient can drive another class of unstable modes which are the ion temperature gradient (ITG) modes. In this multi-instability system, the ion mixing modes can also drive transport fluxes of particle, momentum, and energy, which can enhance or reduce the transport driven by other types of turbulence. Another interesting subject for future works, which further adds to the complexity of this system, is the presence of a parallel flow shear $(\nabla V_\parallel)$. This additional source of free energy can drive parallel shear flow instabilities and can also be a drive mechanism for an inward particle flux.[30] Moreover, in our future works, we study a self-consistent predator-prey type model, taking into account the finite amplitude effects of the flow. As we observed in this work, a finite size flow affects the diffusive relaxation transport fluxes, as well as non-diffusive fluxes of particle and vorticity (momentum). A modified predator-prey model, in which the

effect of finite amplitude zonal flows on the modes is more accurately accounted for, will gives us the opportunity to study the collisionless zonal flow saturation mechanisms and to identify the pathways to shear flow relaxation.

ACKNOWLEDGMENTS

This research was supported by the U.S. Department of Energy Grant Nos. DE-FG02-04ER54738 and DE-SC0008378 and CMTFO. We thank L. Cui, G. R. Tynan, S. C. Thakur, P. Vaezi, Y. Kosuga, S. Kobayashi, M. Malkov, and I. Cziegler for useful discussions.

APPENDIX: DERIVATION OF THE EQUATIONS FOR THE LOCAL DENSITY DEPENDENT, MODIFIED HASEGAWA-WAKATANI SYSTEM

We begin from the ion force-balance relation

$$nm_i\frac{d\mathbf{v}_i}{dt}=en\left(-\nabla\phi+\frac{\mathbf{v}}{c}\times\mathbf{B}\right)-\nabla p_i-\nabla.\mathbf{P}_i, \tag{A1}$$

where p_i is the ion pressure and $\mathbf{P}_i$ is the stress tensor. Assuming cold ions, $T_i \ll T_e$, in the above relation, we will have $\nabla p_i \approx 0$. With the smallness ordering parameter

$$\frac{1}{\omega_{ci}}\frac{d}{dt}\sim\varepsilon\ll 1, \tag{A2}$$

ion velocity to the first order in ε is given by

$$\begin{aligned}\mathbf{v}_i&=\mathbf{v}_E+\mathbf{v}_p+\mathbf{v}_{\text{visc}}\\&=-c\nabla\phi\times\frac{\mathbf{B}}{\mathrm{B}^2}-\frac{c}{\omega_{ci}\mathrm{B}}\frac{d\nabla\phi}{dt}-\frac{1}{nm_i\omega_{ci}}\nabla.\mathbf{P}_i\times\hat{z}\end{aligned} \tag{A3}$$

$\omega_{ci}=eB/m_ic$ is the ion cyclotron frequency and $\hat{z}$ is unit vector pointing in the direction of magnetic field. Current closure relation for a quasi neutral system gives

$$\nabla.\mathbf{J}_\perp=-\nabla_\parallel\mathrm{J}_\parallel. \tag{A4}$$

The perpendicular current comes from the polarization drift current and viscosity of ions $\mathbf{J}_\perp=en\mathbf{v}_p+en\mathbf{v}_{\text{visc}}$

$$\nabla.\mathbf{J}_\perp=e\nabla.[n_0(\mathbf{v}_p+\mathbf{v}_{\text{visc}})], \tag{A5}$$

n_0 is the background density profile ($n=n_0+\delta n$). For the parallel current, we use the Ohm's law

$$\mathrm{J}_\parallel=\frac{e}{m_e\nu_e}\left(\nabla_\parallel p_e+en_eE_\parallel\right)=\frac{eT_e}{m_e\nu_e}\nabla_\parallel\left(n-n_0\hat{\phi}\right), \tag{A6}$$

where $\hat{\phi}=e\phi/T_e$. Now, from Eq. (A4), we have

$$\rho_s^2\nabla.\left[n_0\frac{d}{dt}\nabla\hat{\phi}\right]=\frac{T_e}{m_e\nu_e}\nabla_\parallel^2\left(n-n_0\hat{\phi}\right). \tag{A7}$$

With the spatial dimensions scaled to ρ_s and time scaled to ω_{ci}^{-1}, we rewrite Eq. (A7) as

$$\nabla.\left[n_0\frac{d}{dt}\nabla\hat{\phi}\right]=D_\parallel\nabla_\parallel^2\left(n-n_0\hat{\phi}\right), \tag{A8}$$

where the non-dimensional parallel diffusion coefficient is $D_\parallel=T_e/m_e\nu_e\omega_{ci}$. From the electron continuity equation, we obtain

$$\frac{d}{dt}n=D_\parallel\nabla_\parallel^2\left(n-n_0\hat{\phi}\right). \tag{A9}$$

The linearized form of Eqs. (A8) and (A9) in terms of fluctuations $\delta\hat{n}$ and $\delta\hat{\phi}$ is given by

$$\begin{aligned}&(\partial_t+V_0\partial_y)\nabla.[n_0(x)\nabla\delta\hat{\phi}]+\delta\hat{v}_x\partial_x[n_0\partial_xV_0]\\&\quad=D_\parallel\nabla_\parallel^2(\delta n-n_0\delta\hat{\phi})+\mathrm{D}^\omega\end{aligned} \tag{A10}$$

$$(\partial_t+V_0\partial_y)\delta n+\delta\hat{v}_x\partial_xn_0=D_\parallel\nabla_\parallel^2(\delta n-n_0\delta\hat{\phi})+\mathrm{D}^n, \tag{A11}$$

where $\delta\hat{v}_x=-\partial_y\delta\hat{\phi}$. D^ω and D^n are viscosity related terms, which for non-uniform viscosity coefficients are complicated functions of radius.

Here, we obtain the relation for the positive definiteness of the fluctuation potential enstrophy, for the density dependent, inviscid system. From subtracting Eq. (A10) from Eq. (A11), we obtain

$$\begin{aligned}&(\partial_t+V_0\partial_y)(\delta n-\nabla.[n_0(x)\nabla\delta\hat{\phi}])\\&\quad+\delta\hat{v}_x(\partial_xn_0-\partial_x[n_0\partial_xV_0])=0.\end{aligned} \tag{A12}$$

We assume unstable perturbations of the form given by Eqs. (8) and (9). Now, multiplying Eq. (A12) by $\delta n-\nabla.[n_0(\tilde{x})\nabla\delta\hat{\phi}]$ and averaging over the directions of symmetry, we obtain

$$\frac{\partial}{\partial t}\frac{\langle\delta q_{\mathbf{m}}^2\rangle}{2}=\gamma(\Gamma_{\mathbf{m}}-\partial_x[n_0\mathrm{R}_{\mathbf{m}}])(\partial_xn_0-\partial_x[n_0\partial_xV_0])>0, \tag{A13}$$

where we introduced the averaging

$$\langle\quad\rangle=\frac{1}{L_yL_z}\int_0^{L_y}dy\int_0^{L_z}dz, \tag{A14}$$

$\Gamma_{\mathbf{m}}=\langle\delta\hat{v}_x^{\mathbf{m}}\delta n^{\mathbf{m}}\rangle$ is the particle flux and $\mathrm{R}_{\mathbf{m}}=\langle\delta\hat{v}_x^{\mathbf{m}}\delta\hat{v}_y^{\mathbf{m}}\rangle$ is the Reynolds stress for mode *mn*. Moreover, we can multiply Eq. (A12) by $\delta\hat{v}_x^{\mathbf{m}}$ and average over the symmetric dimensions to obtain

$$\Gamma_{\mathbf{m}}-\partial_x[n_0\mathrm{R}_{\mathbf{m}}]=-\gamma_{\mathbf{m}}\frac{\langle\left(\delta\hat{v}_x^{\mathbf{m}}\right)^2\rangle}{|k_mV_0-\omega_{\mathbf{m}}|^2}(\partial_xn_0-\partial_x[n_0\partial_xV_0]). \tag{A15}$$

Above relation puts the same sign constraint between $\Gamma_{\mathbf{m}}-\partial_x[n_0\mathrm{R}_{\mathbf{m}}]$ and $n_0'-[n_0V_0']'$ as Eq. (A13) did. Moreover, by eliminating $\Gamma_{\mathbf{m}}-\partial_x[n_0\mathrm{R}_{\mathbf{m}}]$ from Eqs. (A13) and (A15), we obtain

$$\frac{\partial}{\partial t}\frac{\langle\delta q_{\mathbf{m}}^2\rangle}{2}=\gamma_{\mathbf{m}}\frac{(\partial_xn_0-\partial_x[n_0\partial_xV_0])^2}{|k_mV_0-\omega_{\mathbf{m}}|^2}\langle\left(\delta\hat{v}_x^{\mathbf{m}}\right)^2\rangle. \tag{A16}$$

[1]L. Schmitz, L. Zeng, T. L. Rhodes, J. C. Hillesheim, E. J. Doyle, R. J. Groebner, W. A. Peebles, K. H. Burrell, and G. Wang, Phys. Rev. Lett. **108**, 155002 (2012).

[2]G. Tynan, M. Xu, P. H. Diamond, J. A. Boedo, I. Cziegler, N. Fedorczak, P. Manz, K. Miki, S. Thakur, L. Schmitz, L. Zeng, E. J. Doyle, G. M. McKee, Z. Yan, G. S. Xu, B. N. Wan, H. Q. Wang, H. Y. Guo, J. Dong, K. Zhao, J. Cheng, W. Y. Hong, and L. W. Yan, Nucl. Fusion **53**, 073053 (2013).
[3]L. A. Charlton, B. A. Carreras, V. E. Lynch, K. L. Sidikman, and P. H. Diamond, Phys. Plasmas **1**, 2700 (1994).
[4]P. H. Diamond, V. Shapiro, V. Shevchenko, Y. B. Kim, M. N. Rosenbluth, B. A. Carreras, K. Sidikman, V. E. Lynch, L. Garcia, P. W. Terry, and R. Z. Sagdeev, Plasma Phys. Controlled Nucl. Fusion Res. **2**, 97 (1993).
[5]B. N. Rogers, W. Dorland, and M. Kotschenreuther, Phys. Rev. Lett. **85**, 5336 (2000).
[6]S. Kobayashi and B. N. Rogers, Phys. Plasmas **19**, 012315 (2012).
[7]S. H. Muller, J. A. Boedo, K. H. Burrell, J. S. deGrassie, R. A. Moyer, W. M. Solomon, D. L. Rudakov, and G. R. Tynan, Phys. Plasmas **18**, 072504 (2011).
[8]U. Stroth, T. Geist, J. P. T. Koponen, P. Z. H. J. Hartfuss, and E. W. A. Team, Phys. Rev. Lett. **82**, 928 (1999).
[9]M. G. Shats and D. L. Rudakov, Phys. Rev. Lett. **79**, 2690 (1997).
[10]J. Boedo, D. Gray, R. Conn, S. Jachmich, G. V. Oost, R. R. Weynants, and T. Team, Czech. J. Phys. **48**, 99 (1998).
[11]T. A. Carter and J. E. Maggs, Phys. Plasmas **16**, 012304 (2009).
[12]S. Zhou, W. W. Heidbrink, H. Boehmer, R. McWilliams, T. A. Carter, S. Vincena, B. Friedman, and D. Schaffner, Phys. Plasmas **19**, 012116 (2012).
[13]S. C. Thakur, C. Brandt, L. Cui, J. J. Gosselin, A. D. Light, and G. R. Tynan, Plasma Sources Sci. Technol. **23**, 044006 (2014).
[14]J. H. Kaplan, Annu. Rev. Biochem. **71**, 511 (2002).
[15]A. A. M. Holtslag and C. H. Moeng, J. Atmos. Sci. **48**, 1690 (1991).
[16]C. G. Falthammar, J. Geophys. Res. **70**, 2503, doi:10.1029/JZ070i011p02503 (1965).
[17]T. J. Birmingh, J. Geophys. Res. **74**, 2169, doi:10.1029/JA074i009p02169 (1969).
[18]J. G. Lyon, Science **288**, 1987 (2000).
[19]A. C. Boxer, R. Bergmann, J. L. Ellsworth, D. T. Garnier, J. Kesner, M. E. Mauel, and P. Woskov, Nat. Phys. **6**, 207 (2010).
[20]M. Schulz and L. J. Lanzerotti, *Particle Diffusion in the Radiation Belts* (Springer-Verlag, 1974).
[21]T. A. Farley, A. D. Tomassian, and M. Walt, Phys. Rev. Lett. **25**, 47 (1970).
[22]F. Wagner and U. Stroth, Plasma Phys. Controlled Fusion **35**, 1321 (1993).
[23]X. Garbet, L. Garzotti, P. Mantica, H. Nordman, M. Valovic, H. Weisen, and C. Angion, Phys. Rev. Lett. **91**, 035001 (2003).
[24]G. T. Hoang, C. Bourdelle, X. Garbet, J. F. Artaud, V. Basiuk, J. Bucalossi, F. Clairet, C. Fenzi-Bonizec, C. Gil, J. L. Segui, J. M. Trave're, E. Tsitrone, and L. Vermare, Phys. Rev. Lett. **93**, 135003 (2004).
[25]C. Bourdelle, Plasma Phys. Controlled Fusion **47**, A317 (2005).
[26]J. Weiland, A. Eriksson, H. Nordman, and A. Zagorodny, Plasma Phys. Controlled Fusion **49**, A45 (2007).
[27]P. H. Diamond, C. J. McDevitt, Ö. D. Gürcan, T. S. Hahm, W. X. Wang, E. S. Yoon, I. Holod, Z. Lin, V. Naulin, and R. Singh, Nucl. Fusion **49**, 045002 (2009).
[28]Z. Yan, M. Xu, P. H. Diamond, C. Holland, S. H. Müller, G. R. Tynan, and J. H. Yu, Phys. Rev. Lett. **104**, 065002 (2010).
[29]B. Coppi and C. Spight, Phys. Rev. Lett. **41**, 551 (1978).
[30]Y. Kosuga, S. Itoh, and K. Itoh, Plasma Fusion Res. **10**, 3401024 (2015).
[31]K. Ida and J. Rice, Nucl. Fusion **54**, 045001 (2014).
[32]P. Diamond, Y. Kosuga, Ö. D. Gürcan, C. McDevitt, T. Hahm, N. Fedorczak, J. Rice, W. Wang, S. Ku, J. Kwon, G. Dif-Pradalier, J. Abiteboul, L. Wang, W. Ko, Y. Shi, K. Ida, W. Solomon, H. Jhang, S. Kim, S. Yi, S. Ko, Y. Sarazin, R. Singh, and C. Chang, Nucl. Fusion **53**, 104019 (2013).
[33]L. Cui, A. Ashourvan, S. C. Thakur, R. Hong, P. Diamond, and G. R. Tynan, "Spontaneous profile self-organization in a simple realization of drift-wave turbulence," Phys. Plasmas (to be published).
[34]L. Cui, G. Tynan, P. Diamond, S. Thakur, and C. Brandt, Phys. Plasmas **22**, 050704 (2015).
[35]M. Wakatani and A. Hasegawa, Phys. Rev. Lett. **59**, 1581 (1987).
[36]M. Wakatani and A. Hasegawa, Phys. Fluids **27**, 611 (1984).
[37]A. Hasegawa and K. Mima, Phys. Fluids **21**, 87 (1978).
[38]C. Rossby, Q. J. R. Meteorol. Soc. **66**, 68 (1940).
[39]W. Horton and A. Hasegawa, Chaos **4**, 227 (1994).
[40]P. Guzdar, J. Drake, D. McCarthy, A. Hassam, and C. Liu, Phys. Fluids B **5**, 3712 (1993).
[41]H. Sugama, M. Wakatani, and A. Hasegawa, Phys. Fluids **31**, 1601 (1988).
[42]B. Carreras, V. Lynch, and L. Garcia, Phys. Fluids B **5**, 1795 (1993).
[43]B. D. Scott, *Plasma Physics and Controlled Nuclear Fusion Research 1994* (IAEA, Vienna, 1995), Vol. III, p. 447.
[44]V. Naulin, Phys. Plasmas **10**, 4016 (2003).
[45]R. Numata, R. Ball, and R. L. Dewar, Phys. Plasmas **14**, 102312 (2007).
[46]B. Scott, Phys. Fluids B **4**, 2468 (1992).
[47]B. Scott, New J. Phys. **4**, 52 (2002).
[48]V. Naulin, A. Nielsen, and J. J. Rasmussen, Phys. Plasmas **12**, 122306 (2005).
[49]Ö. D. Gürcan, P. Diamond, T. Hahm, and Z. Lin, Phys. Plasmas **12**, 032303 (2005).
[50]N. Kasuya, M. Yagi, K. Itoh, and S. Itoh, Phys. Plasmas **15**, 052302 (2008).
[51]M. Sasaki, N. Kasuya, M. Yagi, K. Itoh, Y. Nagashima, S. Inagaki, and S. I. Itoh, Plasma Fusion Res. **8**, 2401113 (2013).
[52]E. Kim and P. H. Diamond, Phys. Plasmas **9**, 4530 (2002).
[53]P. H. Diamond, S.-I. Itoh, K. Itoh, and T. S. Hahm, Plasma Phys. Controlled Fusion **47**, R35–R161 (2005).
[54]A. Shestakov, R. Cohen, J. Crotinger, L. LoDestro, A. Tradini, and X. Xu, J. Comput. Phys. **185**, 399–426 (2002).
[55]W. Horton, T. Tajima, and T. Kamimura, Phys. Fluids **30**(**11**), 3485 (1987).
[56]W. Horton, J. C. Perez, T. Carter, and R. Bengtson, Phys. Plasmas **12**, 022303 (2005).
[57]P. K. Kundu and I. M. Cohen, *Fluid Mechanics* (Academic Press, 2008) Chap. 15, pp. 662–663.